Journal of Alloys and Compounds 488 (2009) 364–369

Contents lists available at ScienceDirect

Journal of Alloys and Compounds

journal homepage: www.elsevier.com/locate/jallcom

Study on the photocatalytic activity of $K_2La_2Ti_3O_{10}$ doped with vanadium (V)

Yahui Yang[a,b,*], Qiyuan Chen[a], Zhoulan Yin[a], Jie Li[a]

[a] College of Chemistry and Chemical Engineering, Central South University, Changsha 410083, China
[b] College of Minerals Processing and Bioengineering, Central South University, Changsha 410083, China

ARTICLE INFO

Article history:
Received 13 March 2009
Received in revised form 28 August 2009
Accepted 28 August 2009
Available online 2 September 2009

Keywords:
$K_2La_2Ti_3O_{10}$
Photocatalytic activity
Hydrogen
The first principles calculation

ABSTRACT

The layered perovskite type oxides, $K_2La_2Ti_3O_{10}$ and V-doped $K_2La_2Ti_3O_{10}$ were prepared by sol–gel method and characterized by different methods such as powder X-ray diffraction, UV–vis diffuse reflectance and X-ray photoelectron spectroscopy. The photocatalytic activity of the catalyst powders for water splitting was investigated with I^- as electron donor under ultraviolet and visible light irradiation, respectively. The electronic structure of the powders has been analyzed by the first principles calculation, showing the photo responses in the visible region and the improvement of the photocatalytic activity of $K_2La_2Ti_3O_{10}$. It is found that V-doped $K_2La_2Ti_3O_{10}$ exhibited higher photocatalytic activity of hydrogen production. When I^- was used as electron donor, the optimum doping concentration of vanadium (V) was found to be 0.015:1 (n_V:n_{Ti}). The average hydrogen production rate of V-doped $K_2La_2Ti_3O_{10}$ under ultraviolet irradiation was 96 μmol/(gcat h) raised by 75% compared with the undoped $K_2La_2Ti_3O_{10}$, the average hydrogen production rate under visible irradiation was 42.2 μmol/(gcat h) raised by 167% compared with the undoped $K_2La_2Ti_3O_{10}$.

1. Introduction

Fujishima and Honda [1] have initiated the development in photocatalysis through the photoelectric conversion of water into hydrogen using TiO_2 since 1972. The photocatalytic splitting of water using oxide semiconductor materials under solar energy is an ideal route to generate hydrogen. In the past several decades, much progress has been made in water photocatalytic cleavage using oxide semiconductor materials to produce hydrogen such as TiO_2 [2–4], niobates [5,6], titanates [7–9], tantalates [10,11], ferrate [12] and vanadate [13]. However, the number of photocatalytic materials known up to now is limited, and note that their activities are quite low. Therefore, a visible-light-sensitive photocatalyst with high activity is still desirable. Compared with the poor activity of visible response photocatalyst, the modification of the ultraviolet-light-sensitive photocatalyst is very useful to utilize solar energy and indoor artificial illuminations. Recently, the layered perovskite photocatalyst $K_2La_2Ti_3O_{10}$ has attracted considerable attention due to its unique properties, for example, optical properties, electrical transport properties, and especially its excellent photocatalytic activity [13–21]. More significantly, $K_2La_2Ti_3O_{10}$ has a lot of derivatives by the replacement of elements of the layer with other elements to show some photo response under visible light irradiation. Inspite of the fact that the transition metal vanadium (V) [22–24] has the possibility to change the energy gap of semiconductor and make it respond to visible light, we have not found any report on $K_2La_2Ti_3O_{10}$ photocatalyst doped with vanadium (V) under visible light irradiation.

In this work, we present the research on the photocatalytic properties of V-doped $K_2La_2Ti_3O_{10}$. The layered perovskite type oxides, $K_2La_2Ti_3O_{10}$ and V-doped $K_2La_2Ti_3O_{10}$ were prepared by sol–gel method and characterized by different methods such as powder X-ray diffraction, UV–vis diffuse reflectance and X-ray photoelectron spectroscopy. The photocatalytic activity for water splitting of the powders was investigated with I^- as electron donor [25,26] under ultraviolet and visible light irradiation, respectively. The electronic structure of the powders was analyzed by the first principles calculation.

2. Experimental

2.1. Preparation of photocatalysts

All the chemical reagents are from Mainland China. Analytical reagents of potassium nitrate (KNO_3, supplied by Bodi Chemical Co. Ltd. in Tianjin), isoproponal ($(CH_3)_2CHOH$, supplied by the Chemical Reagent Plant of Hunan Normal University), lanthanum nitrate ($La(NO_3)_3{\cdot}nH_2O$, supplied by Sinopharm Chemical Reagent Co. Ltd. in Shanghai), potassium iodide (KI, supplied by the Chemical Reagent Plant of Soda Industrial Group Co. Ltd. in Jiaozuo), potassium hydroxide (KOH, supplied by the Chemical Reagent Plant of Hunan Normal University), trichloride ruthenium ($RuCl_3{\cdot}xH_2O$, supplied by Sinopharm Chemical Reagent Co. Ltd. in Shanghai), ammonium vanadate (NH_4VO_3, supplied by Tianjin Chemical Reagent Plant) and chemical reagent of titanium tetrabutyl ($C_{16}H_{36}O_4Ti$, supplied by Lingfeng Chemical Reagent Co. Ltd. in Shanghai) were used in the experiments.

* Corresponding author at: College of Chemistry and Chemical Engineering, Central South University, Yuelu Road, Changsha 410083, China. Tel.: +86 731 88877364; fax: +86 731 88879616.
E-mail address: yangyahui2002@sina.com (Y. Yang).

0925-8388/$ – see front matter © 2009 Elsevier B.V. All rights reserved.
doi:10.1016/j.jallcom.2009.08.136

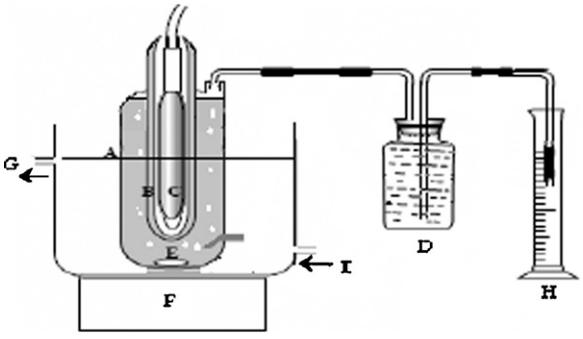

A: Reactor
B: Quartz jacket
C: high-pressure Hg lamp or Xenon lamp
D: Gas collector
E: Magnetic bar
F: Magnetic stirrer
G: Outlet of cooling water
H: Volumetric cylinder
I: Entry of the cooling water

Fig. 1. Device for photocatalytic water splicing. (A: reactor, B: quartz jacket, C: high-pressure Hg lamp or Xenon lamp, D: gas collector, E: magnetic bar, F: magnetic stirrer, G: outlet of the cooling water, H: volumetric cylinder, I: entry of the cooling water).

The $K_2La_2Ti_3O_{10}$ powders were prepared by sol–gel method as reported earlier [27] as follows: solution A was obtained by dissolving the starting materials of 0.02 mol $La(NO_3)_3{\cdot}nH_2O$ and 0.04 mol KNO_3 in 22 mL water and solution B was obtained by dissolving the starting material of 0.03 mol of titanium tetrabutyl ($C_{16}H_{36}O_4Ti$) in 80 mL isopropanol ($(CH_3)_2CHOH$). Solution A was added dropwise to solution B with severe agitation for 5–10 min to get the gelatinous material. The resulted gelatinous material was dried and aged under infrared lamp irradiation for 3–4 h when water and isopropanol were evaporated from the gel. The gel was then crushed and calcined in the presence of air at 950 °C for 4 h, and $K_2La_2Ti_3O_{10}$ powders were thus gained.

Ammonium vanadate (NH_4VO_3) was used as doping precursor and the mol ratio of V to Ti was 0.005:1, 0.01:1, 0.015:1, 0.02:1 and 0.025:1. Ammonium vanadate (NH_4VO_3) was dissolved in solution A and the same operation as above was conducted, V-doped $K_2La_2Ti_3O_{10}$ powders were thus gained.

In order to get high photocatalytic activity, RuO_2 was loaded on the photocatalyst powders using impregnation method [28,29]. The powders were dispersed in $RuCl_3$ aqueous solution by a magnetic stirrer and the solution was heated until water completely volatilized. The powders were ground and oxidized at 500 °C for 5 h in air to make RuO_2 loaded catalyst powders.

2.2. Characterization of photocatalysts

The X-ray diffraction (XRD) patterns of the powders were obtained on a Rigaku D/max2250 VB^+ 18 KW X-ray diffraction analyzer with Cu Kα X-ray source at a scanning rate of 0.1°(2θ)/s. The accelerating voltage and the applied current were 40 kV and 300 mA, respectively. The UV–vis spectroscopy of the powders was recorded on a Lambda 900 UV–vis spectrometer with labsphere integrating sphere. The XPS spectroscopy of the powders was recorded on an X-ray photoelectron spectrometer with Mg Kα X-ray source (1253.6 eV, 16 mA × 12 kV). The evolved hydrogen was determined by a SP-2305 gas phase chromatography instrument with thermal conductivity detector, Ar carrier, 5A molecular sieve column, and the sampling volume was 100 μL.

2.3. Photocatalytic experiments

The photocatalytic water splitting reaction was carried out in a self-made tube-shaped quartz reactor including three layers connected with gas collecting devices, and water was used as the external circulation cooling and wind as the internal cooling (see Fig. 1). The reaction temperature was kept at 25 ± 0.2 °C by controlling the external circulation water in the water jacket of reactor throughout the experiment. The light source was a 250 W high-pressure Hg lamp, of which the radiative wavelength was about 300–400 nm, the intensity of illumination was 15×10^3 μW/(cm^2) and the average luminous flux was 75×10^4 lx. The photocatalyst powders (1.0 g) were dispersed in 600 mL aqueous solution by a magnetic stirrer and 5.6 g KI was added to pure water after boiling for 30 min to remove the dissolved oxygen. KOH was added to control the pH of the solution at 11.8. Before irradiation, the cell was deaerated with nitrogen for about 30 min. The evolved gases were determined with a TCD gas chromatograph and its volume was collected and confirmed by drainage method.

Table 1
Influence of V-dopant concentration on the lattice parameter of $K_2La_2Ti_3O_{10}$ photocatalysts.

	Vanadium concentration (n_V:n_{Ti})					
	0	0.005:1	0.01:1	0.015:1	0.02:1	0.025:1
Lattice parameter (nm)						
x,*y*	0.387104	0.387522	0.38728	0.387283	0.387506	0.387526
z	2.978414	2.977352	2.97274	2.970018	2.969043	2.968241

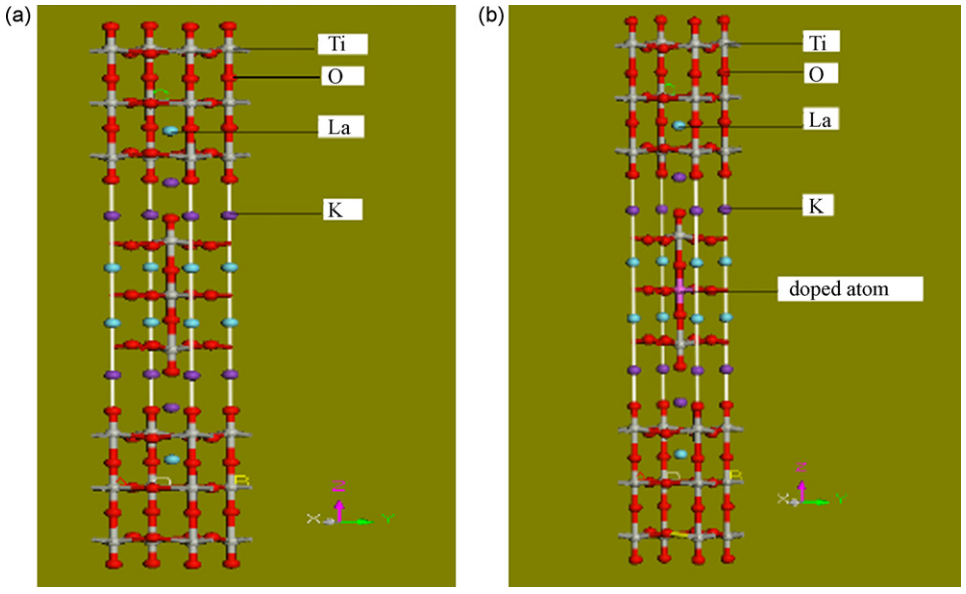

Fig. 2. Supercell model of $K_2La_2Ti_3O_{10}$ (a) and V-doped $K_2La_2Ti_3O_{10}$ (b) considered in the present work.

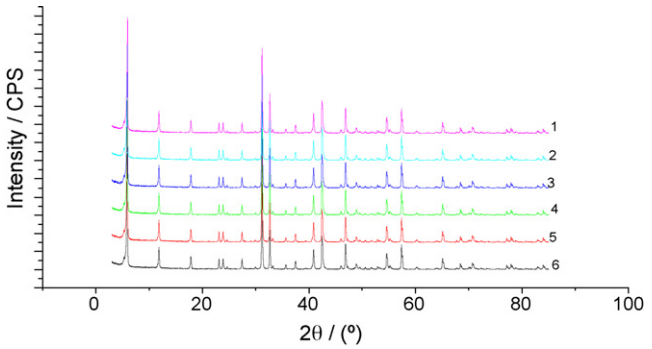

Fig. 3. Influence of vanadium concentration on the XRD patterns of $K_2La_2Ti_3O_{10}$ photocatalysts. n_V:n_{Ti} = (1) 0.025:1; (2) 0.02:1; (3) 0.015:1; (4) 0.01:1; (5) 0.005:1; (6) 0.

In order to study the photocatalytic activity on irradiation with visible light, the 250 W high-pressure Hg lamp was substituted by a 250 W Xenon lamp whose average luminous flux was 15×10^4 lx. The Xenon lamp has about the same characteristic spectrum with sunlight.

2.4. Methods and theoretical models of the first principle calculations

All the calculations in this paper were performed using the CASTEP software package in Material Studio 3.2, which belongs to the calculation working station of College of Chemistry and Chemical Engineering, Central South University. CASTEP is a quantum mechanics program based on density functional theory (DFT). It adopts the plane-wave pseudo-potential approach. The particle–field interaction is substituted by a pseudo-potential, electronic wave functions are expanded in terms of a discrete plane-wave basis set, and the exchange and correlation potential are described with the local density approximation (LDA) and generalized gradient approximation (GGA). It is the most precise method used for calculation of electronic structure at present.

$K_2La_2Ti_3O_{10}$ has an ideal hexagonal body-centered perovskite structure. It belongs to the space group of *I*4/*mmm* and symmetry of C4v. Its lattice constant is that $x = y = 0.387104$ nm, $z = 2.978414$ nm and $\alpha = \beta = \gamma = 90°$. In the present calculations, the ultrasoft pseudo-potential based on the LDA is employed. The cutoff energy of a plane-wave is set at 300 eV. The theoretical model is shown in Fig. 2.

The position of vanadium atom is constructed in terms of the changes of lattice constant of $K_2La_2Ti_3O_{10}$. Because of the change (see Table 1) of *z* and steric factors, the substituting of V atoms for Ti atoms of the interlayer octahedron of [TiO_6] in $K_2La_2Ti_3O_{10}$ is reasonable.

3. Results and discussion

3.1. Characterization of the powders

Fig. 3 shows the XRD patterns of the powders. Table 1 shows the influence of vanadium concentration on the lattice parameter of $K_2La_2Ti_3O_{10}$ photocatalysts. Fig. 2 and Table 1 show that addition

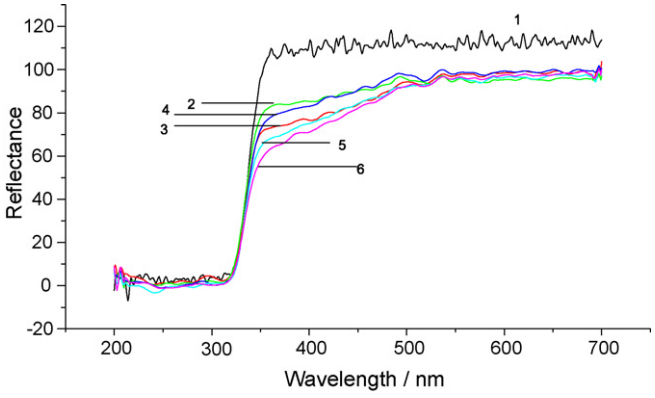

Fig. 4. Dependence of vanadium concentration on the diffuse reflection spectra of $K_2La_2Ti_3O_{10}$ photocatalysts. n_V:n_{Ti} = (1) 0.025:1; (2) 0.02:1; (3) 0.015:1; (4) 0.01:1; (5) 0.005:1; (6) 0.

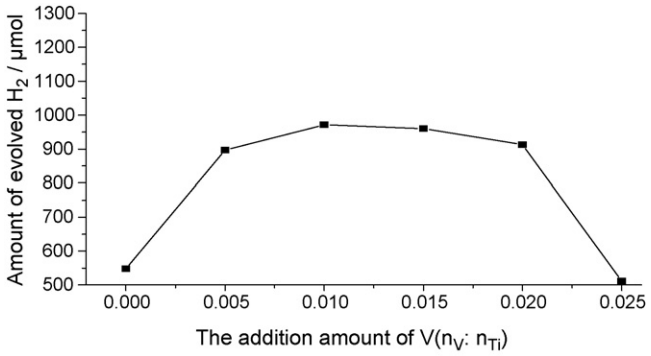

Fig. 5. Dependence of vanadium concentration on the photocatalytic activity of $K_2La_2Ti_3O_{10}$ for hydrogen production under ultraviolet light radiation.

of vanadium does not change the crystal structure of $K_2La_2Ti_3O_{10}$ and the catalyst powders have perfect crystal structure. However the dopant changes the lattice parameter of $K_2La_2Ti_3O_{10}$, especially the value of *z*, indicating that V atoms are possibly inserted into the crystal of $K_2La_2Ti_3O_{10}$. Table 1 also shows that the value of *z* diminished with the increasing of vanadium concentration, which possibly results from the smaller ionic radius of V (0.059 nm) compared with that of Ti (0.068 nm) [30].

Fig. 4 shows the diffuse reflectance spectra of the powders. Sharp UV absorptions are identified near 310 nm, and by extrapolating the reflection edge the experimental band gap energy is estimated to be ca. 4.0 eV [31,32], which is consistent with the theoretical band gap energy. But the V-doped catalysts show different absorption behavior in visible light range near 400–500 nm which means that it is favorable for the improvement of the photocatalytic activity under visible light irradiation.

3.2. Influence of vanadium concentration on the photocatalytic activity of $K_2La_2Ti_3O_{10}$

The photocatalytic activity of the powders was compared under ultraviolet and visible light radiation using I^- as electron donor. Fig. 5 and Table 2 show the effect of vanadium concentration on the photocatalytic activity of $K_2La_2Ti_3O_{10}$ under ultraviolet light radiation. In a reasonable range, the addition of vanadium can improve the photoactivity of $K_2La_2Ti_3O_{10}$. The optimum doping concentration of vanadium was found to be 0.01:1 and 0.015:1 (n_V:n_{Ti}), the hydrogen production rates were 97 and 96 μmol/(gcat h) which were raised by 77 and 75% compared with undoped $K_2La_2Ti_3O_{10}$. When the doping concentration of vanadium exceeded a given value, the dopant becomes a promising trap and will capture the photo-generated electron. As a result of that, the catalysts will easily lose its photoactivity for hydrogen production.

Fig. 6 and Table 2 show the influence of vanadium concentration on the photocatalytic activity of the powders under visible light radiation. The optimum doping concentration of vanadium was found to be 0.015:1 (n_V:n_{Ti}), and the average hydrogen production rate was 42.2 μmol/(gcat h) which was raised by 167% compared with the undoped $K_2La_2Ti_3O_{10}$.

Table 2
Dependence of vanadium concentration on the photocatalytic activity of $K_2La_2Ti_3O_{10}$ for hydrogen production.

	Vanadium concentration (n_V:n_{Ti})					
	0	0.005:1	0.01:1	0.015:1	0.02:1	0.025:1
Rate of hydrogen evolution (μmol/(gcat h))						
UV	54.8	89.7	97	96	91	51
Vis	15.8	16.4	18	42.2	26.4	0

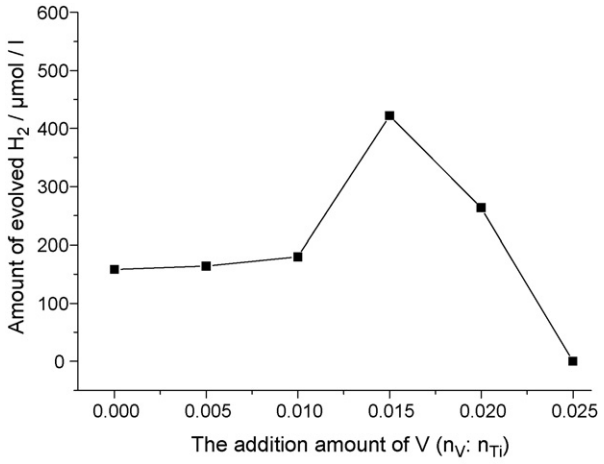

Fig. 6. Dependence of vanadium concentration on the photocatalytic activity of $K_2La_2Ti_3O_{10}$ for hydrogen production under visible light radiation.

3.3. Reason for the improvement of the photoactivity of $K_2La_2Ti_3O_{10}$ doped with vanadium

Fig. 7 shows the O1s-XPS spectra of the obtained powders. It is clear that there exist mainly two types of surface oxygen in the catalyst powders, i.e lattice oxygen (α) whose binding energy is 529.3 eV and adsorption oxygen (β) whose binding energy is 530.9 eV. The oxygen defects will affect the photoactivity of the catalyst powders for water splitting. The spectra

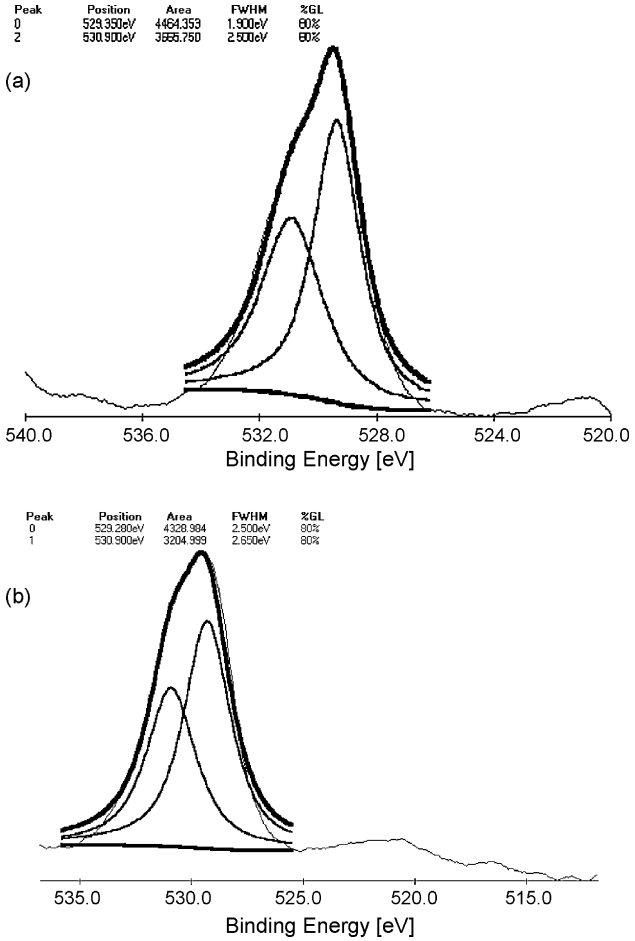

Fig. 7. O1s-XPS spectra of $K_2La_2Ti_3O_{10}$ (a) and V-doped $K_2La_2Ti_3O_{10}$ (b).

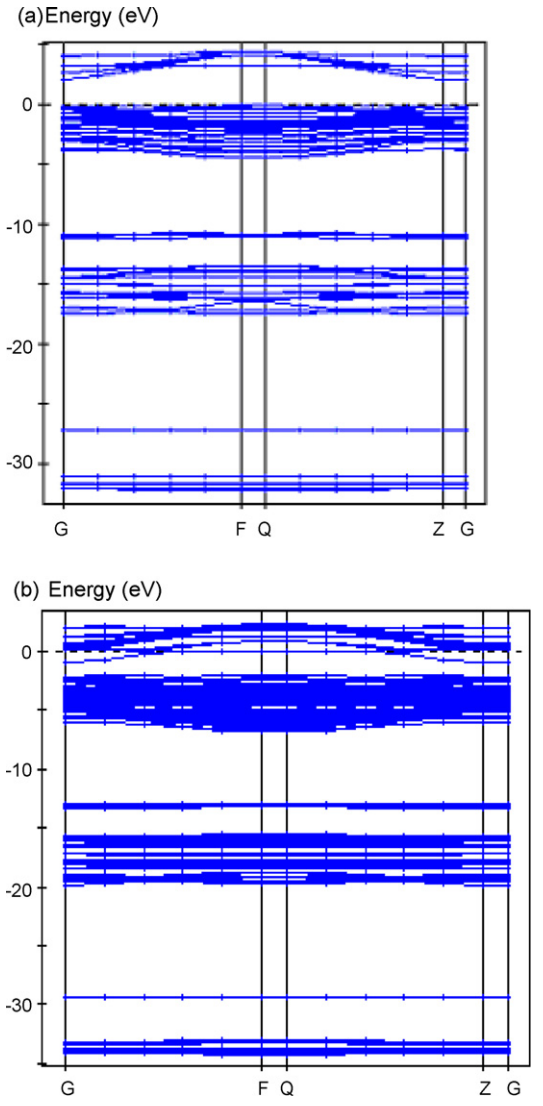

Fig. 8. Calculated band structure of $K_2La_2Ti_3O_{10}$ (a) and V-doped $K_2La_2Ti_3O_{10}$ (b).

in Fig. 7 illustrates that the ratio of lattice oxygen (α) was 55% for $K_2La_2Ti_3O_{10}$ whereas 42.6% for V-doped $K_2La_2Ti_3O_{10}$. At the same time, the ratio of adsorption oxygen (β) was 45% for $K_2La_2Ti_3O_{10}$ and 57.4% for V-doped $K_2La_2Ti_3O_{10}$, showing that V-doped $K_2La_2Ti_3O_{10}$ has lower lattice oxygen (α) ratio [33,34] and higher oxygen vacancy ratio. The oxygen vacancies of the catalyst powders belong to positive centers and are easily exicited to the conduction band as donor band level which is at the bottom of conduction band of the catalyst powders. Due to higher oxygen vacancy ratio, there are more photo-generated electrons for V-doped $K_2La_2Ti_3O_{10}$ which can jump easily to the conduction band compared with the undoped $K_2La_2Ti_3O_{10}$. At the same time, the oxygen vacancies can inhibit the recombination of photo-generated electrons and holes and thus improve the photoactivity of V-doped $K_2La_2Ti_3O_{10}$.

Doping of $K_2La_2Ti_3O_{10}$ with V cation results in increased concentration of electrons in the conduction band, as illustrated by the following defect site reaction [35]:

$$V_2O_5 \rightarrow 2V_{Ti}{}^{+} + 4O_0{}^{*} + 1/2O_2 + 2e^{-} \quad (1)$$

In the above expression, $V_{Ti}{}^{+}$ is the V^{5+} substituted for crystal lattice Ti^{4+} and $O_0{}^{*}$ is the crystal lattice O^{2-}. The increase of the

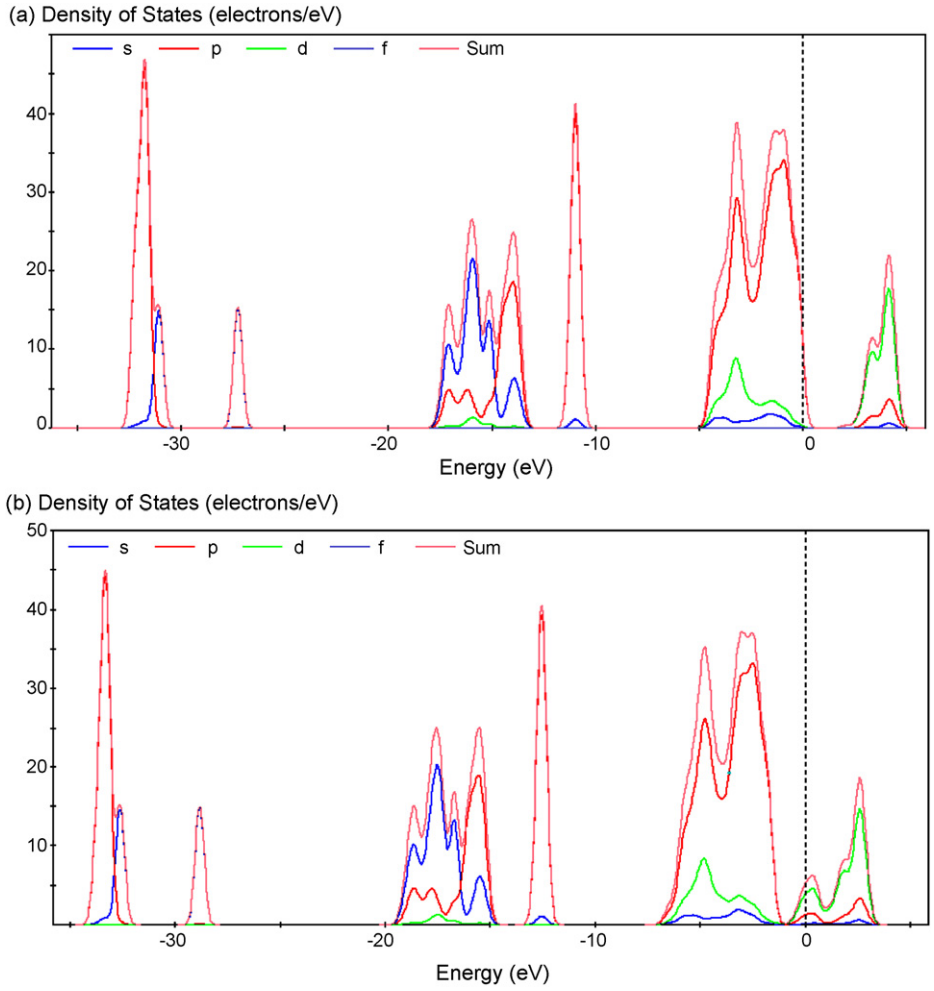

Fig. 9. Partial DOS of $K_2La_2Ti_3O_{10}$ (a) and (b) V-doped $K_2La_2Ti_3O_{10}$ (b).

electron concentration in the conduction band results in the lowering of the work function or an upward shift of the Fermi energy level is also expected [36], and, consequently, a cathodic shift of the flat band potential toward negative values with respect to the NHE potential. The reducing ability of photo-generated electrons is also strengthened with the improvement of the photoactivity of V-doped $K_2La_2Ti_3O_{10}$.

As mentioned above, the energy level and the band gap of the semiconductor can play a crucial role in determining its photocatalytic activity. In order to show the effect of V-doping on the electronic structure of $K_2La_2Ti_3O_{10}$, the band structure and partial density of states (PDOS) of $K_2La_2Ti_3O_{10}$ are also calculated for comparison. The calculation results are shown in Figs. 7 and 8.

As shown in Figs. 8 and 9, the band structure of photocatalysts consists of valence band and conduction band. Obviously, the hybridization of Ti 3d electron orbits with O 2p electron orbits forms the energy band of photocatalysts. The conduction band mainly consists of Ti 3d electron orbits, and valence band mainly of O 2p electron orbits. The lower valence band zone (less than −10 eV) is not considered in the research because of its weak interaction with the conduction band. Fig. 8 illustrates that there is an energy gap between the valence band and the conduction band, and the photocatalysts are indirect band gap semiconductor. The bottom of the conduction band is at G site of Brillouin zone, and the top of valence band is at Q site. The value of the band gap is about 2.1 eV, which is smaller than the experimental value of about 4.0 eV. The reason for this disagreement may be the well-known shortcoming of the theoretical frame of DFT-LDA.

Figs. 8 and 9 illustrate that $K_2La_2Ti_3O_{10}$ doped with vanadium results in the hybridization of Ti and V 3d electron orbits with O 2p electron orbits and an upward shift of the Fermi energy level into the conduction band of $K_2La_2Ti_3O_{10}$. The hybridization of V 3d electron orbits with O 2p electron orbits forms a new localized energy level and the catalyst is easily excited with lower energy, which is consistent with the absorption behavior in visible light range as illustrated in Fig. 3. This may explain our experimental results that there is an optimum visible-light absorption for higher hydrogen rate.

4. Conclusions

In summary, V-doped $K_2La_2Ti_3O_{10}$ exhibited higher photocatalytic activity of hydrogen production. The optimum doping concentration of vanadium was found to be 0.015:1 (n_{Zn}:n_{Ti}), the average hydrogen production rates were 96 μmol/(gcat h) under ultraviolet irradiation and 42.2 μmol/(gcat h) under visible light irradiation which were raised by 75 and 167% compared with the undoped $K_2La_2Ti_3O_{10}$, respectively. The hybridization of V 3d electron orbits with O 2p electron orbits forms a new localized energy level and the catalyst is easily excited with lower energy to improve the photoactivity of $K_2La_2Ti_3O_{10}$ for water splitting.

Acknowledgements

This research was financially supported by the National High-Tech. Research and Development Program of China (No. 2002AA327140), Hunan Provincial Natural Science Foundation of China (No. 08JJ3022)

References

[1] A. Fujishima, K. Honda, Nature 238 (1972) 37.
[2] S.C. Moon, H. Mametsuka, S. Tabata, E. Suzuki, Catal. Today 58 (2000) 125.
[3] R. Dholam, N. Patel, M. Adami, A. Miotello, Int. J. Hydrogen Energy 34 (2009) 5337.
[4] W. Chatpaisalsakul, O. Mekasuwandumrong, J. Panpranot, C. Satayaprasert, P. Praserthdam, J. Ind. Eng. Chem. 15 (2009) 77.
[5] H.Y. Lin, T.H. Lee, C.Y. Sie, Int. J. Hydrogen Energy 33 (2008) 4055.
[6] Y.F. Huang, Y.L. Wei, L.Q. Fan, M.L. Huang, J.M. Lin, J.H. Wu, Int. J. Hydrogen Energy 34 (2009) 5318.
[7] W. Shangguan, A. Yoshida, Int. J. Hydrogen Energy 24 (1999) 425.
[8] S. Ikeda, K. Hirao, S. Ishino, M. Matsumura, B. Ohtani, Catal. Today 117 (2006) 343.
[9] J.H. Yan, Y.R. Zhu, Y.G. Tang, Q.Z. Shu, J. Alloys Compd. 472 (2009) 429.
[10] Z.G. Zou, J.H. Ye, K. Sayama, H. Arakawa, Nature 414 (2001) 625.
[11] Y.C. Chiou, U. Kumar, J.C.S. Wu, Appl. Catal. A: Gen. 1357 (2009) 73.
[12] H.H. Yang, J.H. Yan, Z.G. Lu, X. Cheng, Y.G. Tang, J. Alloys Compd. 476 (2009) 715.
[13] D.N. Ke, T.Y. Peng, L. Ma, P. Cai, P. Jiang, Appl. Catal. A: Gen. 350 (2008) 111.
[14] S. Ikeda, M. Hara, J.N. Kondo, K. Domen, H. Takahashi, T. Okubo, M. Kakihana, Chem. Mater. 10 (1998) 72.
[15] T. Takata, K. Shinohara, A. Tanaka, M. Hara, J.N. Kondo, K. Domen, J. Photochem. Photobiol. A 106 (1997) 45.
[16] C.T.K. Thaminimulla, T. Takata, M. Hara, J.N. Kondo, K. Domen, J. Catal. 196 (2000) 362.
[17] L.L. Zhang, J. Yang, W.G. Zhang, L.D. Lu, X.J. Yang, X. Wang, Chin. J. Inorg. Chem. 19 (2003) 1217.
[18] Y.W. Tai, J.S. Chen, C.C. Yang, B.Z. Wan, Catal. Today 97 (2004) 95.
[19] Z.W. Tong, G.Z. Zhang, S. Takagi, T. Shimada, H. Tachibana, H. Inoue, Chem. Lett. 34 (2005) 632.
[20] W.Q. Cui, L. Liu, L.R. Feng, C.H. Xu, Z.J. Li, S.L. Lv, F.L. Qiu, Sci. China Ser. B. 49 (2006) 162.
[21] Y.F. Huang, J.H. Wu, Y.L. Wei, J.M. Lin, M.L. Huang, J. Alloys Compd. 456 (2008) 364.
[22] D.E. Gu, B.C. Yang, Y.D. Hu, Catal. Commun. 9 (2008) 1472.
[23] J.M. Xie, X.M. Lu, M. Chen, G.Q. Zhao, Y.Z. Song, S.S. Lu, Dyes Pigments 77 (2008) 43.
[24] P. Shah, D.S. Bhange, A.S. Deshpande, M.S. Kulkarni, N.M. Gupta, Mater. Chem. Phys. 117 (2009) 399.
[25] R. Abe, K. Sayama, K. Domen, H. Arakawa, Chem. Phys. Lett. 344 (2001) 339.
[26] R. Abe, K. Sayama, H. Arakawa, Chem. Phys. Lett. 371 (2003) 360.
[27] Y.H. Yang, Q.Y. Chen, Z.L. Yin, J. Li, Chin. J. Nonferrous Metals 17 (2007) 642.
[28] C.Y. Wang, C.Y. Liu, T. Shen, Chem. Res. Chin. Univ. 19 (1999) 2013.
[29] L.L. Amy, G.Q. Lu, T.Y. John, Chem. Rev. 95 (1995) 735.
[30] J.A. Dean, Lang's Hand Book of Chemistry, McGraw-Hill, Inc., 1991, p. 30, Chapter 4.
[31] K.H. Chung, D.C. Park, J. Mol. Catal. A: Chem. 29 (1998) 53.
[32] M. Machida, X.W. Ma, H. Taniguchi, J. Yabunaka, T. Kijima, J. Mol. Catal. A: Chem. 155 (2000) 131.
[33] Y.Q. Wang, L. Zhang, H.M. Cheng, J.M. Ma, Chem. J. Chin. Univ. 21 (2000) 958.
[34] X.X. Fu, Q.H. Yang, L.X. Sang, Chem. Res. Chin. Univ. 23 (2002) 283.
[35] M.Z. Su, The Introduction of Solid State Chemistry, Beijing University Press, Beijing, 1987, p. 99, Chapter 3.
[36] K.E. Karakitson, X.E. Verykios, J. Phys. Chem. 97 (1993) 1184.